

Supporting Information for:

Star-shaped Oligo(*p*-phenylenevinylene) Substituted Hexaarylbenzene: Purity, Stability and Chiral Self- assembly

*Željko Tomović, Joost van Dongen, Subi J. George, Hong Xu, Wojciech Pisula, Philippe Leclère,
Maarten M.J. Smulders, Steven De Feyter, E. W. Meijer and Albertus P. H. J. Schenning*

1. General Methods

Nuclear Magnetic Resonance spectroscopy (NMR). ¹H NMR and ¹³C NMR spectra were recorded in CDCl₃ and CD₂Cl₂ at 25.0 °C on a Varian Mercury Vx (400 MHz for ¹H and 100 MHz for ¹³C). Chemical shifts (δ) are given in ppm relative to tetramethylsilane, which was used as internal standard. Abbreviations used are s = singlet, d = doublet, t = triplet and m = multiplet.

Mass spectroscopy (MS). MALDI-TOF MS spectra were measured on a Perspective DE Voyager spectrometer utilising a 2-[(2E)-3-(4-*tert*-butylphenyl)-2-methylprop-2-enylidene]malononitrile (DCTB), α-cyano-4-hydroxycinnamic acid (CHCA) or dithranol matrix.

Gel permeation chromatography (GPC). Analytical GPC was carried out in chloroform using Plgel (5 μm, 500 Å, 300 X 7.5 mm) or Plgel (5 μm, 10⁴ Å, 300 X 7.5 mm) columns and in THF using Plgel single pore size (100 Å) 30 cm columns, with a particle size of 3 μm connected in series with a SPD-M10Avp photodiode array UV/Vis detector.

Recycling gel permeation chromatography (rGPC). Preparative rGPC was carried out in chloroform at a flow rate of 3.5 mL/min, with a Jaigel 2,5 H preparative column (20 mm i.d. x 60 mm length) (Japan Analytical Industry Co., Ltd.) connected to a dual wavelength ($\lambda = 254$ and 420 nm) UV/Vis detector (Shimadzu).

Infrared spectroscopy (IR). Infrared spectra were recorded on a Perkin Elmer Spectrum One UATR FT-IR spectrophotometer.

Optical spectroscopy. UV-vis and Circular Dichroism measurement were performed on a Jasco J-815 spectropolarimeter where the sensitivity, time constant and scan rate were chosen appropriately. Corresponding temperature dependent measurements were performed with a PFD-425S/15 Peltier-type temperature controller with a temperature range of 263-383 K and adjustable temperature slope. Fluorescence measurements were performed on a Edinburgh Instruments FS920 double-monochromator luminescence spectrometer using a Peltier-cooled red-sensitive photomultiplier.

Atomic Force Microscopy (AFM). AFM images were recorded under ambient conditions using a Digital Instrument Multimode Nanoscope IV operating in the Tapping mode regime. Microfabricated silicon cantilever tips (NS) with a resonance frequency of approximately 300 kHz and a spring constant of about 50 Nm^{-1} were used. Samples for AFM study were prepared by drop casting **3** solution under a solvent atmosphere on freshly cleaved silicon wafer or highly oriented pyrolytic graphite (HOPG).

DSC: Thermal analysis was carried out using a Perkin Elmer Differential Scanning Calorimetry Pyris 1 with a Pyris 1 DSC autosampler and a Perkin Elmer CCA7 cooling element under a nitrogen atmosphere with heating and cooling rates of $10 \text{ }^\circ\text{C/min}$.

TGA: Thermal gravimetric analysis (TGA) data was collected under nitrogen on a Perkin-Elmer TGA 7 apparatus.

X-ray. The 2D-WAXS experiments were performed by means of a rotating anode (Rigaku 18 kW) X-ray beam with a pinhole collimation and a 2D Siemens detector. A double graphite monochromator for the Cu-K α radiation ($\lambda = 0.154 \text{ nm}$) was used.

Polarization microscopy. A Zeiss microscope equipped with polarizing filters and equipped with a Hitachi KP-D50 Colour digital CCD camera was used in order to investigate the optical textures of the compounds. The samples were sandwiched between two glass slides and then thermally treated on a Linkam hotstage fitted with a Linkam TMS 91 temperature controller.

Scanning Tunneling Microscopy (STM). All experiments were performed at 20–22 °C and were performed using a Discoverer scanning tunneling microscope (Topometrix, Santa Barbara, USA) along with an external pulse/function generator (model HP 8111 A) with negative sample bias. Pt/Ir STM tips were prepared by electrochemical etching from Pt/Ir wire (80%/20%, diameter 0.2 mm) in a 2N KOH/6N NaCN solution in water.

Prior to imaging the compounds under investigation were dissolved in 1-phenyloctane (Aldrich) at a concentration of approximately 0.1 mg/ml to 1 mg/ml, and a drop of this solution was applied on a freshly cleaved surface of HOPG (grade ZTB, Advanced Ceramics Inc., Cleveland, USA). Then, the STM tip was immersed into the solution. The bright (dark) contrast refers to a high (low) current (constant-height mode). The bias voltage was applied to the sample in such a way that at negative bias voltage, electrons tunnel from the sample to the tip.

2. Materials.

(*E,E,E*)-4-[4-{4-(3,4,5-Tridodecyloxystyryl)-2,5-bis[(*S*)-2-methylbutoxy]styryl}-2,5-bis[(*S*)-2-methylbutoxy]-styryl]phenylbromide (**1**) was synthesized according to the literature procedure.^{S1} All solvents were of AR quality and chemicals were used as received. Deuterated chloroform and methylene chloride were obtained from Cambridge Isotope Laboratories and used as received. Bio-Beads S-X1 were obtained from Bio-Rad Laboratories. All synthetic procedures were performed in an inert atmosphere of dry argon.

2: 435 mg (0,32 mmol) of **1** and 20 mg (0.017 mmol) Pd(PPh₃)₄ were dissolved in 6 mL dry toluene under an argon atmosphere. 94.2 mg (0.156 mmol) Bis(tributylstannyl)acetylene was added dropwise and the mixture was refluxed for 24 h. After cooling, the solvent was removed under reduced pressure and the residue purified by column chromatography (silica gel, hexane/dichloromethane = 3/2) to afford 225 mg (54% yield) **2**, as an orange solid.

¹H-NMR (400 MHz, CDCl₃, 25 °C): δ = 0.89 (t, 18H, CH₃), 1.02 (t, 24H, CH₃), 1.12 (m, 24H, CH₃), 1.20-1.55 (m, 108H, CH₂), 1.60-1.90 (m, 28H, CH₂), 1.90-2.05 (m, 8H, CH), 3.80-4.05 (m, 28H, OCH₂), 6.75 (s, 4H, Ar-H), 7.04 (d, J=16 Hz, 2H, Ar-CH=CH), 7.11 (s, 2H, Ar-H), 7.13 (s, 2H, Ar-H), 7.16 (d, J=16.4 Hz, 2H, Ar-CH=CH), 7.20 (s, 4H, Ar-H), 7.39 (d, J=16 Hz, 2H, Ar-CH=CH), 7.53 (d, J=16 Hz, 2H, Ar-CH=CH), 7.45-7.60 (m, 12H, Ar-CH=CH, Ar-H) ppm.

¹³C-NMR (100 MHz, CDCl₃, 25 °C): δ = 11.75, 11.84, 11.89, 14.47, 17.14, 17.23, 23.05, 26.49, 26.73, 26.76, 29.73, 29.76, 29.80, 29.99, 30.02, 30.07, 30.10, 30.12, 30.71, 32.28, 35.34, 35.45, 35.51, 69.44, 73.90, 74.40, 74.55, 74.77, 74.84, 91.00, 105.45, 109.93, 110.25, 110.78, 111.27, 122.36, 122.88, 123.21, 124.81, 126.71, 127.22, 127.72, 128.26, 128.32, 128.96, 132.25, 133.59, 138.37, 138.52, 151.33, 151.46, 151.52, 151.79, 153.60 ppm.

IR (UATR): ν (cm⁻¹) = 3060, 2957, 2921, 2853, 1579, 1506, 1467, 1423, 1389, 1342, 1245, 1204, 1119, 1046, 1009, 967, 916, 852, 819, 762, 722, 695, 668.

MALDI-TOF MS (calculated for C₁₇₄H₂₇₀O₁₄ = 2586): *m/z* = 2586 [M]⁺.

3: 150 mg (0.058 mmol) of **2** was dissolved in 7 mL 1,4-dioxane under an argon atmosphere and 4 mg (0.012 mmol) of Co₂(CO)₈ was added. The mixture was refluxed for 7 h and the solvent removed *in vacuo*. The residue was purified by column chromatography on silica gel (hexane/dichloromethane = 6/4), preparative size-exclusion chromatography (Bio-Beads, SX1) with tetrahydrofuran as eluent and finally recycling gel permeation chromatography (chloroform as eluent, six injections, each had 5-9

cycles, separation was monitored at 254, 340, 437, and 500 nm) to afford 85 mg (57% yield) of **3** as an orange solid.

$^1\text{H-NMR}$ (400 MHz, CD_2Cl_2 , 25 °C): δ = 0.80-1.15 (m, 198H, CH_3), 1.20-1.40 (m, 288H, CH_2), 1.40-1.75 (m, 84H, CH_2), 1.75-1.85 (m, 36H, CH_2), 1.85-2.00 (m, 24H, CH), 3.70-3.95 (m, 48H, OCH_2), 3.95-4.05 (m, 36H, OCH_2), 6.71 (s, 12H, Ar-H), 6.90-7.20 (m, 60H, Ar- $\text{CH}=\text{CH}$, Ar-H), 7.30-7.45 (2d, $J=16$ Hz, 8H and 4H, Ar- $\text{CH}=\text{CH}$), 7.45-7.55 (m, 12H, Ar-H) ppm.

$^{13}\text{C-NMR}$ (100 MHz, CD_2Cl_2 , 25 °C): δ = 11.41, 14.02, 16.66, 16.69, 16.73, 22.83, 26.28, 26.43, 26.50, 26.53, 29.51, 29.54, 29.58, 29.76, 29.86, 29.90, 32.08, 35.25, 35.28, 69.05, 73.54, 74.11, 74.27, 74.43, 104.7, 109.49, 109.84, 110.27, 110.51, 122.39, 122.58, 122.69, 125.08, 126.75, 127.33, 127.38, 128.41, 128.64, 132.03, 133.27, 135.08, 138.02, 140.19, 140.45, 151.07, 151.20, 151.23, 151.27, 153.41 ppm.

IR (UATR): ν (cm^{-1}) = 3058, 2957, 2921, 2852, 1579, 1505, 1466, 1422, 1388, 1340, 1252, 1200, 1153, 1118, 1044, 1009, 965, 916, 852, 815, 760, 720, 696.

MALDI-TOF MS (calculated for $\text{C}_{522}\text{H}_{810}\text{O}_{42}$ = 7758): m/z = 7757 [M] $^+$.

Side product.

$^1\text{H-NMR}$ (400 MHz, CD_2Cl_2 , 25 °C): δ = 0.80-1.16 (m, 132H, CH_3), 1.20-2.00 (m, 288H, CH_2 , CH), 3.80-3.95 (m, 32H, OCH_2), 3.96-4.04 (m, 24H, OCH_2), 6.74 (s, 8H, Ar-H), 7.00-7.58 (m, 56H, Ar- $\text{CH}=\text{CH}$, Ar-H) ppm.

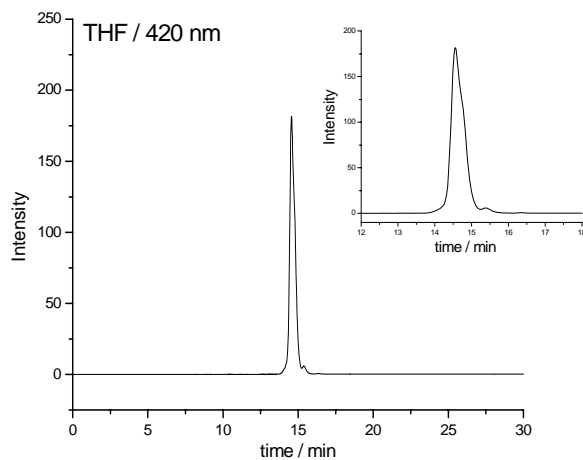
$^{13}\text{C-NMR}$ (100 MHz, CD_2Cl_2 , 25 °C): δ = 11.41, 13.99, 16.73, 22.81, 26.26, 26.49, 26.52, 29.49, 29.58, 29.78, 29.83, 29.88, 32.05, 35.25, 69.03, 73.53, 74.08, 74.27, 74.43, 104.69, 109.52, 109.85, 110.27, 110.75, 122.37, 122.64, 126.82, 127.24, 127.33, 128.68, 130.64, 133.26, 138.02, 151.23, 153.40 ppm.

IR (UATR): ν (cm^{-1}) = 3059, 2958, 2922, 2853, 1707 (C=O), 1579, 1505, 1466, 1422, 1387, 1341, 1244, 1202, 1153, 1117, 1045, 1010, 964, 916, 852, 810, 773, 722, 697.

MALDI-TOF MS (calculated for $\text{C}_{349}\text{H}_{540}\text{O}_{29} = 5200$): $m/z = 5203$ $[\text{M}]^+$

3. Figures

a)



b)

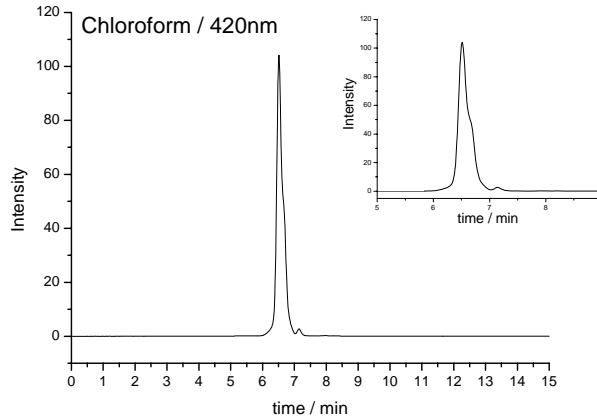
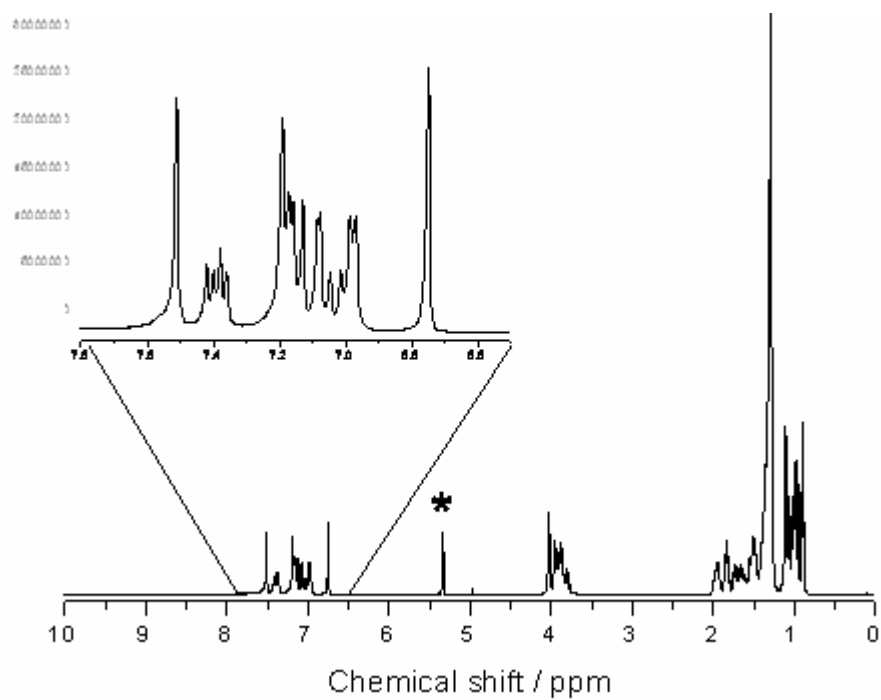


Figure S1. GPC traces with THF and chloroform as eluent, respectively, of **3** obtained after purification by column chromatography and Bio-Beads column chromatography, before purification using recycling gel permeation chromatography.

a)



b)

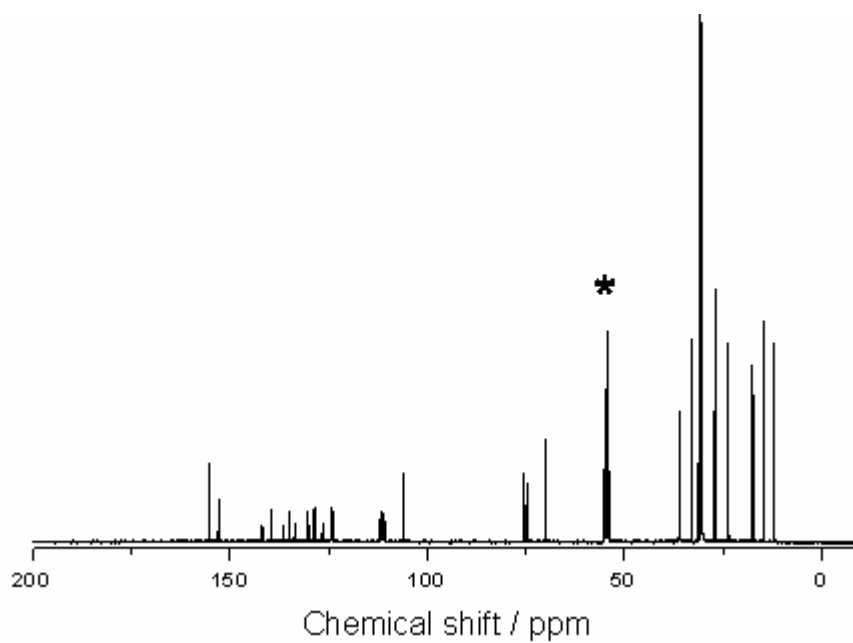


Figure S2. (a) ^1H and (b) ^{13}C NMR spectra of purified **3** in dichloromethane- d_2 (*) at 25 °C.

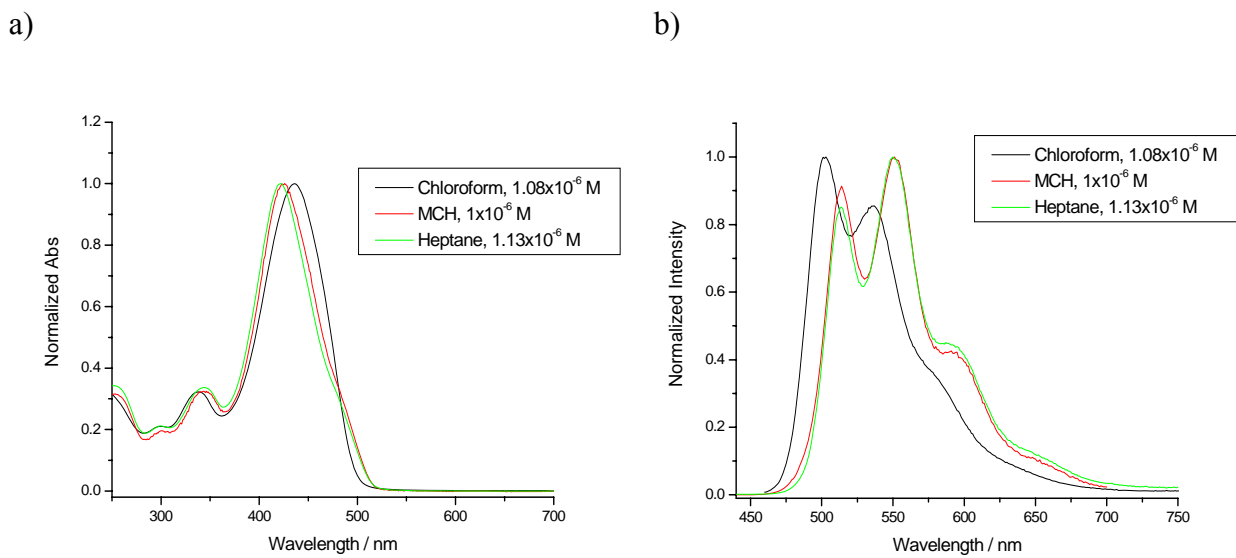


Figure S3. a) UV-Vis and b) PL measurements of **3** in chloroform, MCH and heptane.

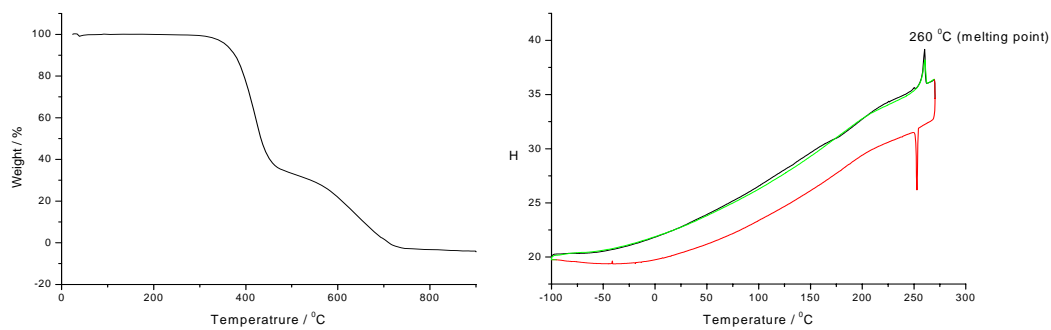


Figure S4. TGA analysis (left) and differential scanning calorimetry scans of **3** (10 °C/min) (right).

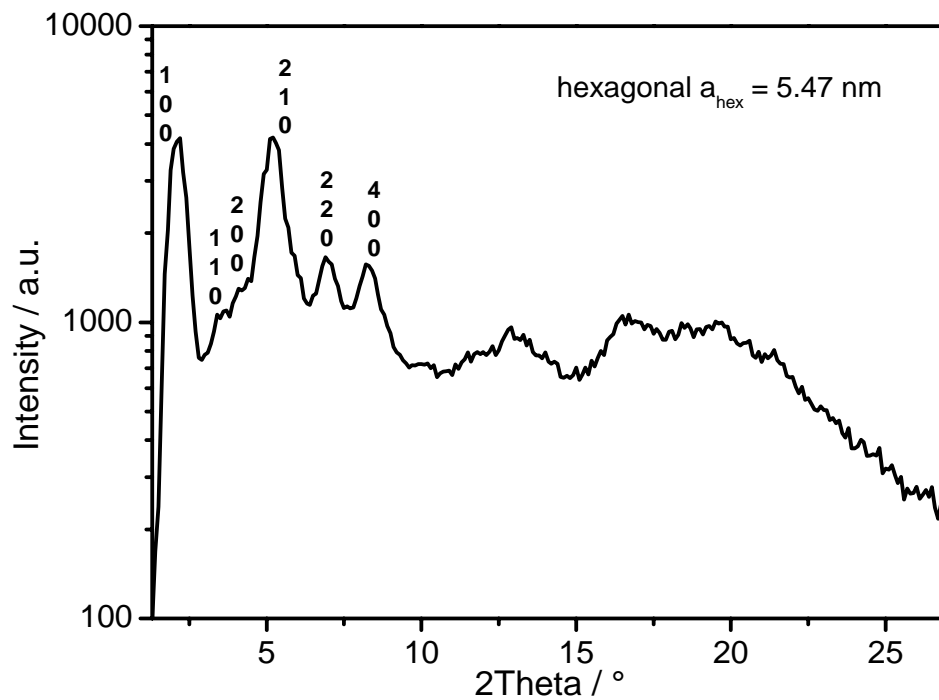


Figure S5. Equatorial scattering intensity distribution as a function of the scattering angle, the reflections are assigned by the Miller's indices, measured for **3**.

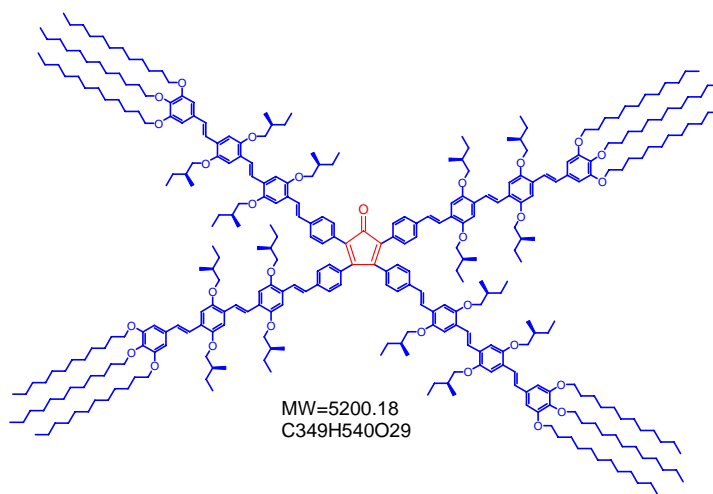
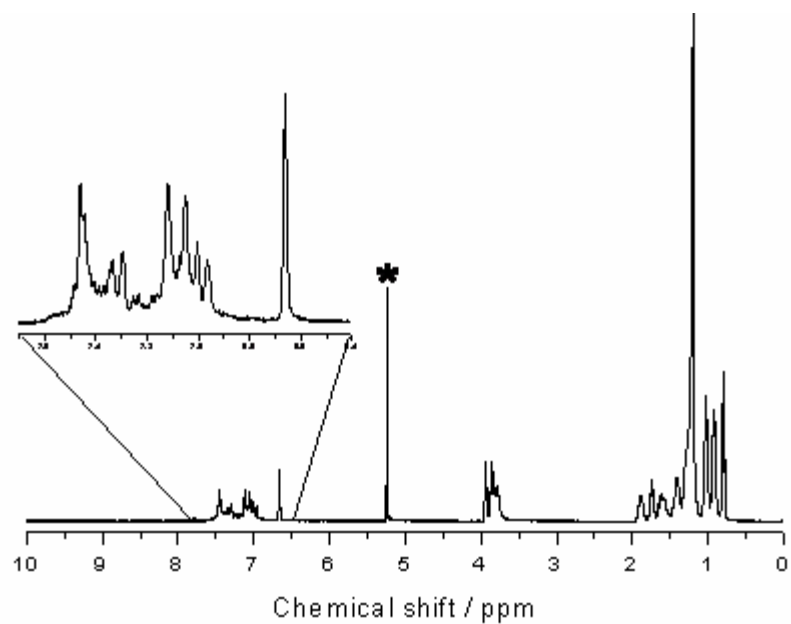


Figure S6. Proposed structure of side product obtained during cyclotrimerization of **2**.

a)



b)

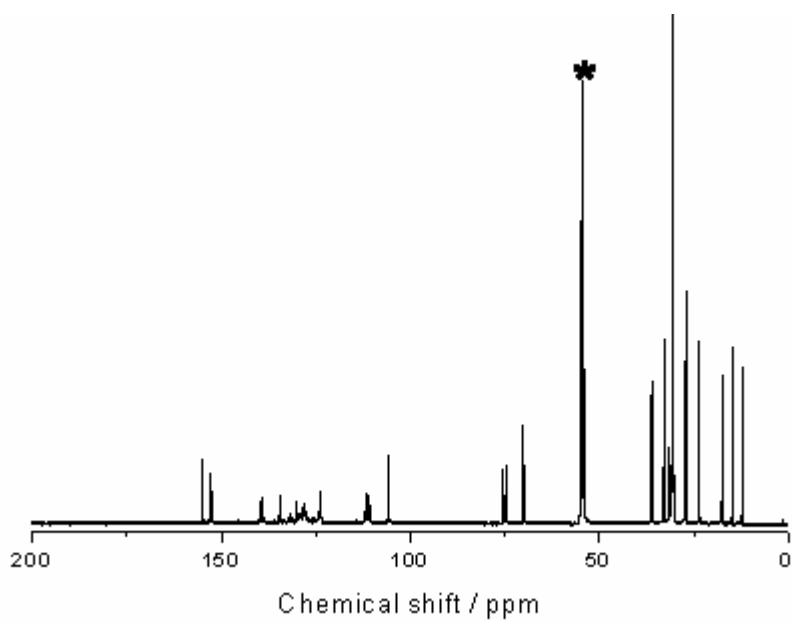


Figure S7. (a) ^1H and (b) ^{13}C NMR spectra of side product (obtained during cyclotrimerization of **2**, purified by rGPC) in dichloromethane- d_2 (*) at 25 °C.

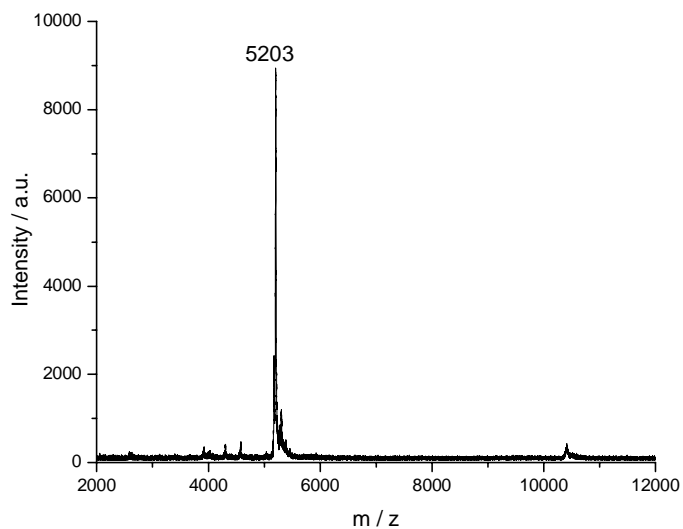
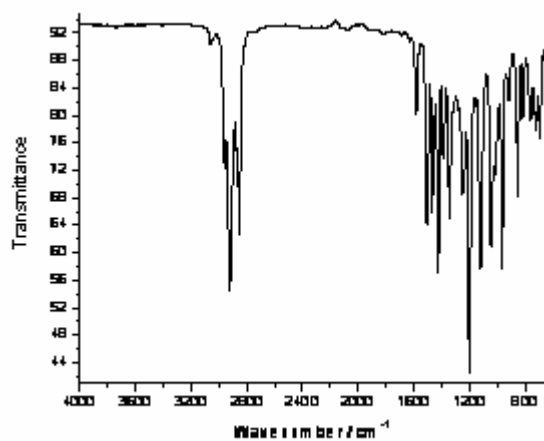


Figure S8. MALDI-TOF MS spectrum of the side product (obtained during cyclotrimerization of **2**), after purification by rGPC.

a)



b)

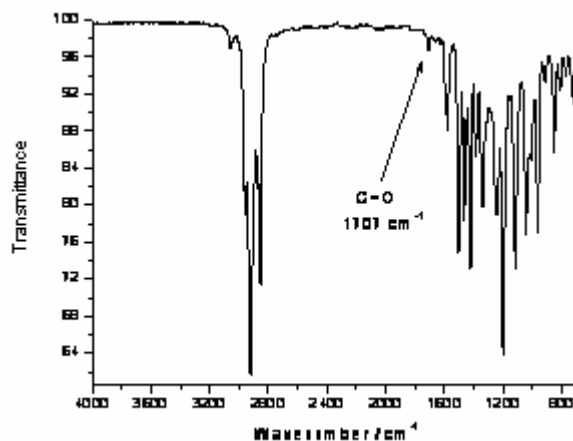


Figure S9. IR spectra of (a) star-shaped OPV (**3**), and (b) side product

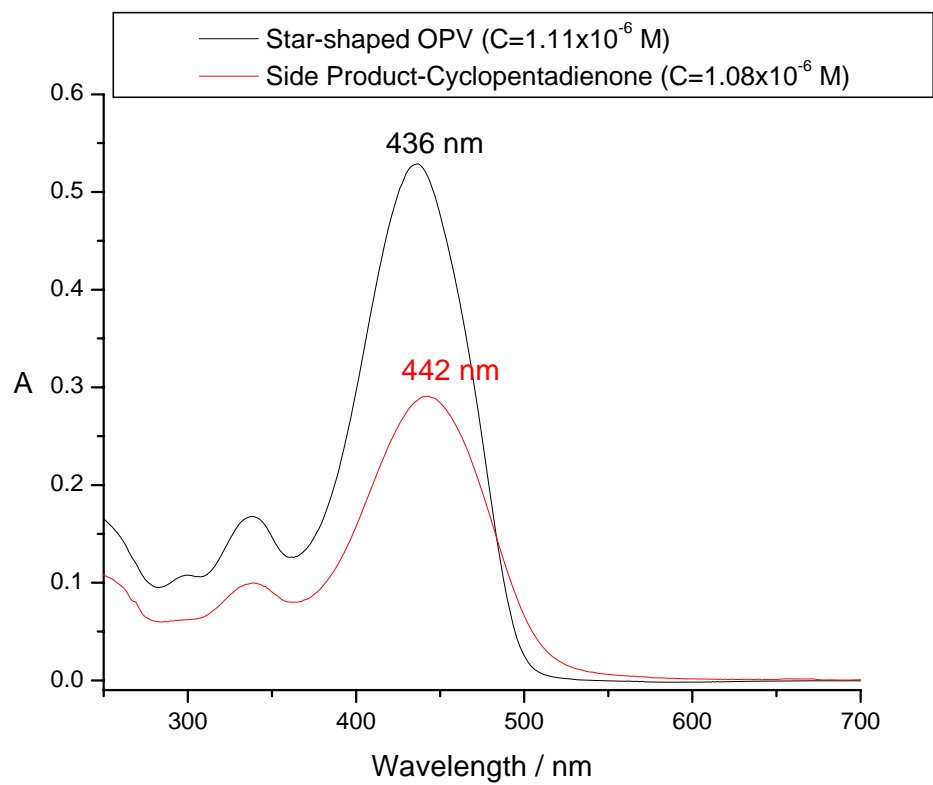


Figure S10. UV-Vis of star-shaped OPV (**3**) and side product in chloroform.

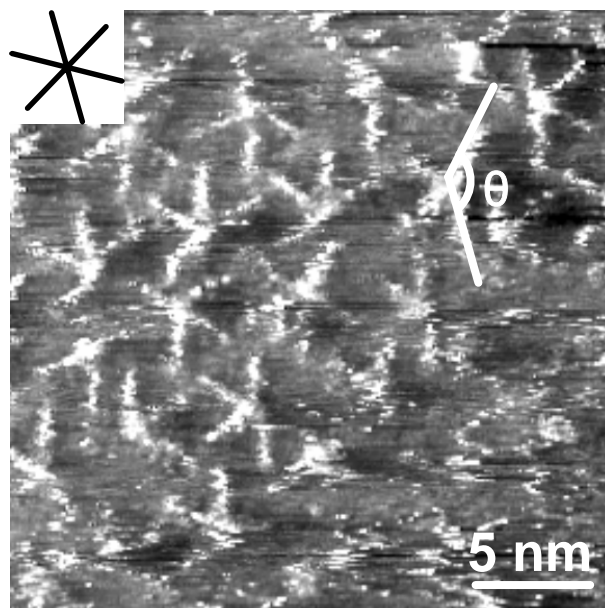


Figure S11. STM image of the side product, formed during the synthesis of **3**, after applying a drop of the 1-phenyloctane solution (roughly 1 mg/ml) on the basal plane of a freshly cleaved highly oriented pyrolytic graphite piece. The bright rods are attributed to the conjugated OPV units. Typically, four of these bright rods are linked to a central point which is in line with the predicted molecular structure. The patterns are disordered which is not surprising giving the peculiar symmetry of these molecules. The maximum angle between two OPV units ranges between 160° and 180° , which is also in line with the anticipated cyclopentadienone structure.

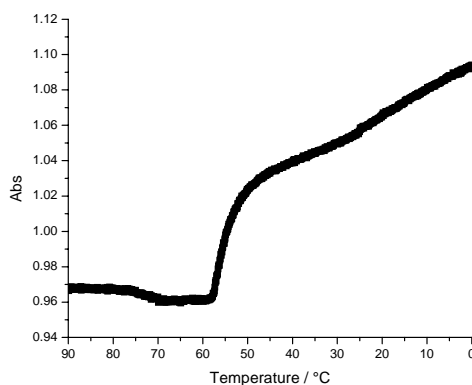


Figure S12. Melting curve of **3** in MCH (2.5×10^{-6} M) obtained by monitoring absorption intensity at 500 nm ($dT/dt = 12$ °C/hr).

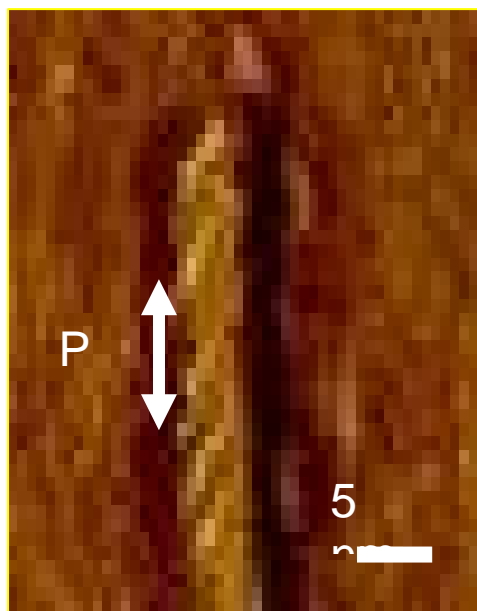


Figure S13. Determination of the pitch of the chiral fibrils formed by **3**. Tapping mode phase images of **3** (1.06×10^{-6} M) deposited from heptane solutions on silicon wafer.

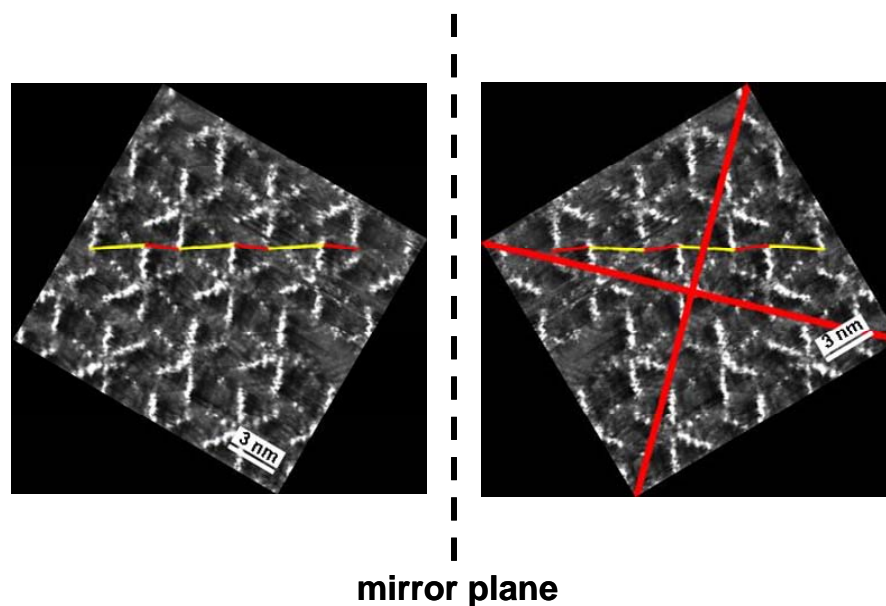


Figure S14. Left: STM image of **3** at the 1-phenyloctane /graphite interface. Right: Software induced mirror image of the STM image on the left. The longer yellow and shorter red lines connect the terminal phenyl groups of similarly oriented OPV units along unit cell vector b . Experimentally, the molecular arrangement in the right figure has never been observed.

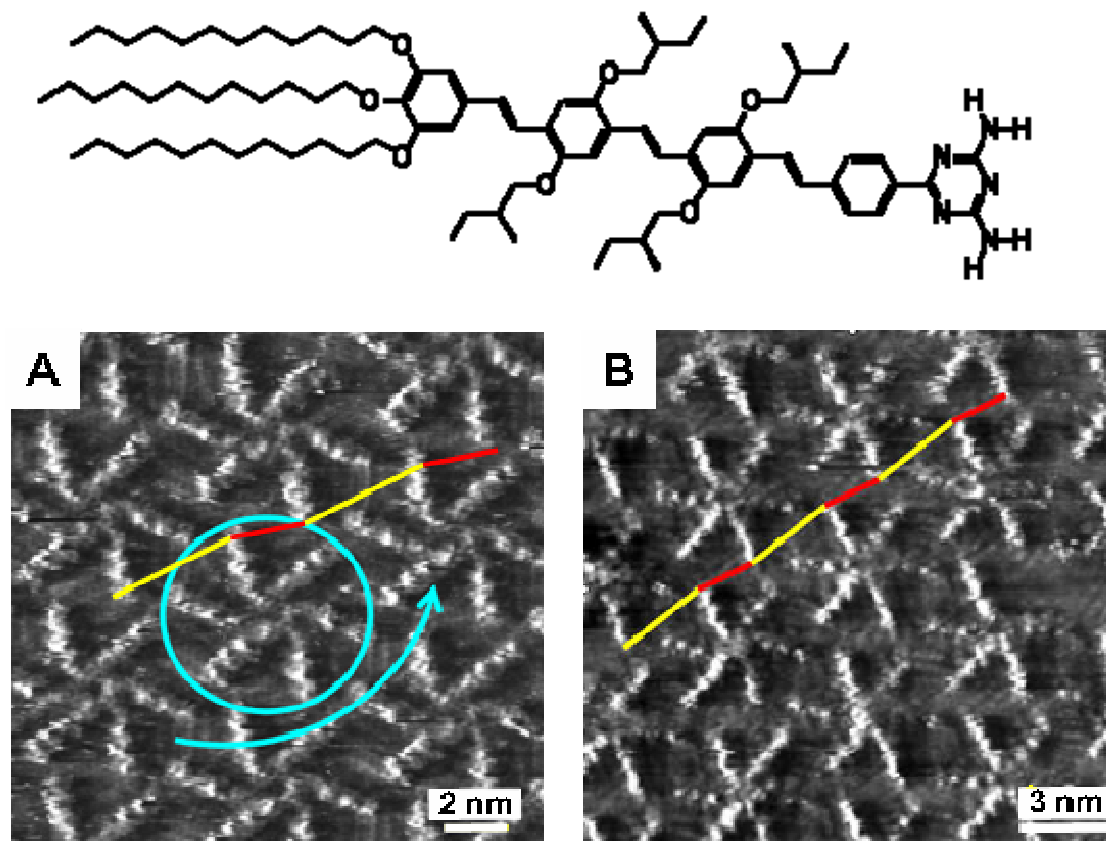


Figure S15. A) STM-image of the OPV-oligomer (top) at the 1-phenyloctane/graphite interface.^{S2} B) STM-image of **3** at the 1-phenyloctane /graphite interface. The longer yellow and shorter red lines connect the terminal phenyl groups of similarly oriented OPV units along unit cell vector *b*. The blue arrow in A indicates the virtual rotation direction of the supramolecular cyclic hexamer.

Complete reference 6b:

Schenning, A. P. H. J.; Jonkheijm, P. Hoeben, F. J. M.; van Herrikhuyzen, J.; Meskers, S. C. J.; Meijer, E. W.; Herz, L. M.; Daniel, C.; Silva, C.; Phillips, R. T.; Friend, R. H.; Beljonne, D.; Miura, A.; De Feyter, S.; Zdanowska, M.; Uji-ie, H.; De Schryver, F. C.; Chen, Z.; Würthner, F.; Mas-Torrent, M.; den Boer, D.; Durkut, M.; Hadley, P. *Synth. Met.* **2004**, *147*, 43–48.

S1 Schenning, A.P.H.J.; Fransen, M.; van Duren, J. K. J.; van Hal, P. A.; Janssen, R. A. J.; Meijer, E. W. *Macromol. Rapid Commun.* **2002**, *23*, 271-275.

S2 a) Jonkheijm, P.; Miura, A.; Zdanowska, M.; Hoeben, F.J.M.; De Feyter, S.; Schenning, A. P. H. J.; De Schryver F.C.; Meijer, E.W *Angew. Chem. Int Ed.* **2004**, *43*, 74-78; b) Miura, A.;

Jonkheijm, P.; De Feyter, S.; Schenning, A. P. H. J.; Meijer, E. W.; De Schryver, F. C. *Small* **2005**, 131-137.